THEORETICAL AND EXPERIMENTAL STUDY OF CONICAL TUBE HYDROFORMING WITH ONE-SIDED AXIAL FEEDING

UDC:621.744
Original scientific paper https://doi.org/10.18485/aeletters.2022.7.3.3

Yusra Jasim[1], Ghazwan Alwan[1], Tahseen Othman[1*]

[1]Mechanical Engineering Department, Faculty of Engineering, Tikrit University, Iraq

Abstract:
Hydroforming has gained increasing attention in the manufacturing industry in recent years due to the demand for fast yet reliable production for parts, the applications of which accept a wide range of dimensional tolerances. In this study, tube hydroforming in conical dies has been analyzed. The study consists of two parts: computer simulations and experimental work. The simulation results were utilized to find the load paths which produce successful hydroforming for the selected tube specimens. Twelve load paths were identified and implemented with two friction coefficients and three pressure ranges. During the simulation process, the tubes were given an end movement that ranged from a sealing distance to twice that distance. The experimental work was implemented to verify some of the simulation results. The results showed that the best hydroforming limit was reached when the axial feeding was twice as much as the sealing distance. Also, the maximum amount of deformation rate happens shortly after the specimen-die interface starts having relative motion, and it is at its slowest when the hydroforming reaches the fully-formed specimen's shape.

ARTICLE HISTORY
Received: 12.06.2022.
Accepted: 26.09.2022.
Available: 30.09.2022.

KEYWORDS
Conical Tube Hydroforming (THF), Finite Element, Corner filling, axial feeding, plastic deformation

1. INTRODUCTION

Hydroforming is a metal forming process in which a tubular blank or a piece of sheet is placed in a closed die and imposed to conform to the shape of the die's cavity by applying hydraulic pressure. Tube Hydroforming (THF) can be classified into feed-driven and expansion-driven. The distinction between the two types emerges from whether there is a significant application of material feeding by means of mechanical tools, which is required in cases of complex geometries. THF process utilization assists in designing and optimizing parts for transportation vehicles, such as engine exhaust manifolds, engine cradles, chassis, and many other tubular parts [1-7].

The product from THF process is distinguished from products that are produced by other classical means by the reduction of the production steps, improving the product strength, and reducing the weight and cost of the equipment. On the other hand, the high tooling cost is a disadvantage for the process, especially the sealing mechanisms [8], as well as the un-deterministic nature of the resulting dimensional tolerances [9]. Several parameters affect the hydroforming process related to the material, geometry, and loading pattern. The material parameters include mechanical properties of tube material, such as elongation, tensile strength, strain hardening rate, etc., while process parameters represent the load path which is, generally speaking, the loading of internal pressure and the amount of axial feeding. Also, the die's geometric configuration and the status of the lubrication at the specimen – die interface have significant impact on the outcome [10,11].

The definition of a successful hydroforming process is that the product takes the shape of the die after implementing a pre-determined loading path with the expected shape and mechanical specifications. Several works have shown that

*CONTACT: T. Othman, e-mail: tahseentaha@tu.edu.iq

controlling the loading path between the hydraulic pressure and the axial feeding simultaneously improves the tube shaping capabilities without failures [12-14]. By loading paths, it is meant the internal pressure and the forced axial movement of the lower edge of the tube. The paths' choice and timings affect the final product's shape and mechanical characteristics [15-17]. If tube hydroforming is performed under proper loading conditions, a successful product result. If, however, the process is done under improper forming conditions, failures, such as buckling, bursting, or wrinkling may occur. Bursting happens when the material's hardening reaches its limit, as well as the internal pressure keeps increasing at the same time. When it comes to the improper feeding rate, the wrinkling or buckling failure modes may happen if more tube material is provided due to axial feeding than what can be compensated by the material deformation from the increase of internal pressure, and the material's ductility was found to be a major contributor to it. Additionally, the failure could happen via a combination of all the events above if the internal pressure and tube-end feeding are not correctly applied [18,19].

One of the significant parameters that influence the quality of the product is the amount of friction between the die and the specimen during the hydroforming process. The friction at the specimen-die interface usually causes a non-uniform distribution in terms of shear stress, as well as variation in the thickness of the formed product along its length [11,20-22]. The degree to which the friction is present depends on the geometrical features and the loading conditions between moving surfaces since hydroforming is an active process of deformation in different directions.

Hydroforming studies have investigated the related parameters such as geometry, friction, and loading path. When it comes to special cases with simple geometrical shapes, some studies considered square dies in order to have some insight into the major parameters affecting the hydroforming. Orban and Hu [21] presented analytical models for the planar tube hydroforming in square die and used the models for parametric studies. In their study, they investigated several parameters, including friction and geometric configurations. Also, a detailed analysis was presented on the timing of the loading steps as well as the adhering (sticking), which helps in understanding the formability limit. It was found that friction has the most significant impact on the variation of thickness of the wall of the product. Later, the analytical models were validated numerically and experimentally on regular and irregular polygon dies. Yang and Ngaile [23] presented a planar tube hydroforming analytical model. In the model, several polygon shapes were considered for the hydroformed products. Also, several parameters were taken in the study, such as wall thinning, corner filling, and plate bending. The results were compared with ones from finite element analysis and experimental results. The results showed the potential benefit of such models in providing preliminary insight into hydroforming prior to performing extensive research with other tools.

One of the significant limiting features of hydroforming is corner filling (acute angle filling). During the design process of the specimen-die loading path, special care must be taken for the corners in the desired shape of the product. Several studies focused on corner filling, and one of the main conclusions is that increasing the hydraulic pressure may not be enough to fill the corners as a solo acting factor [9,24]. In research [24] and based on previous works, a proposal for an experimental validation procedure for a constitutive model with excessive feeding for the worked conical specimen was presented. It was pointed out that this type of geometry is formidable in terms of the need for a high rate of feeding in order to have complete products where there are acute angles with the relative difficulty of corner filling. During the tests, the thickness distribution was measured and compared against the model's limit and capacity. However, friction was not considered in the simulation. Their results showed the possibility of having a strong and accurate prediction for the hydroforming after completing the verification and taking measurements for the deformation and strains at different stages and multiple points. Furthermore, in research [9], two plastic stability criteria were utilized to study the limiting strains in tube hydroforming. Moreover, the cases were also considered for finite element analysis, then compared with experimental tests of conical dies for the consideration of corner filling. It was found that although the FE analysis agrees well with the two criteria, disagreements with the experimental work were reported between the free bulge and constraining die hydroforming.

From the above, it may be concluded that choosing the proper loading path for both the internal pressure and axial feeding rates have

influenced the outcome in a direct manner, especially on corner fillings, being the critical components of the process and limiting factor for any die design. Hence, in this study, a conical tube hydroforming process was performed to investigate the choice of loading path on the resulting specimens. The shape of the die was chosen to focus on the corner filling since it is a challenging aspect of any hydroforming process. The analysis was performed in a plane where the die's corner lies in a plane parallel to the tube's longitudinal axis since there is still no analytical model for this type of analysis (Fig. 1) [9,24]. The study has two parts; in the former one, ANSYS simulation of 2D model was considered in order to determine the best possible loading path via an iterative procedure. This gave the advantage of reducing the cost of prototyping and experimentation [25]. In the later part, experimental work was conducted on copper tubes in order to study and observe the resulting specimens in terms of the generated shape as well as to validate the simulation results with qualitative assessment.

The results show that in order to form the tubes into the geometry of the die and to get the best corner filling in a conical die, the axial feeding would be twice as much as the sealing feeding. This has to be done in coordination with the increase in internal pressure. Also, the study showed that the process is susceptible to the adhering effect between the outer surface of the specimen and the die at the beginning of the deformation, and that it exists regardless of the friction value. This results in the inner part of the tube being thinner than the outer one.

2. MATERIALS AND METHODS

2.1 Finite element modeling

The finite element analysis has been used extensively by researchers to investigate the hydroforming process because of its versatility in covering the physical aspects with verifiable accuracy [26-28]. Fig. 1 shows a schematic diagram of one-side axial feeding conical THF. The process was modeled using ANSYS, a finite element analysis software package. Since the problem is axisymmetric, a 2D version was adapted to save computational time with quasi-static analysis. Plane183 eight-node element was used to model the deformable tubular body with elastic-plastic material behavior, whereas a Target169 element was used to model the die. By using the contact 172 (3-node element), the tube-die interface was modeled. Two values of coefficient of friction, μ, were utilized in this study; 0.03 for dry condition, while 0.045 when mineral oil was used as a lubricant. These results were experimentally determined for the samples from ring tests as this is a practical test configuration given the nature of the hydroforming deformation [29]. Furthermore, it is worthy to point out that small one mm-radius arcs replaced the two sharp corners at the die entrance to prevent the material adhering and obstruction. In regard to the mesh, four layers of elements in the thickness direction were chosen. The material properties were represented as power law as follows,

$$\bar{\sigma} = K\bar{\varepsilon}^{n} . \quad (1)$$

Where K is the strength coefficient, n is the strain hardening exponent, $\bar{\sigma}$ the true representative stress, and $\bar{\varepsilon}$ is the true representative strain.

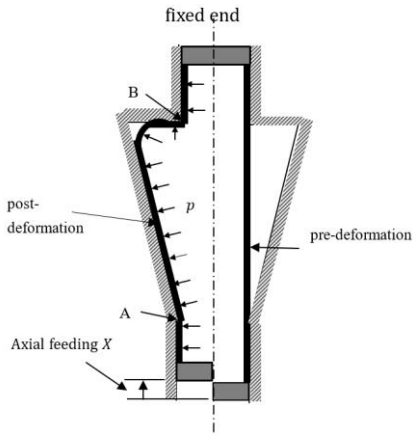

Fig. 1. Conical Tube Hydroforming

The boundary conditions were applied to the model. With respect to Fig. 1, The upper end has fixed nodes in all DOF, while the lower ones were given axial, inward motion in accordance with the loading paths. The inner nodes were loaded with pressure evenly on the surface in a concurrent manner with lower edge motion. The resulting shape was reached once the lower edge movement stops, and there is no more deformation happening as the internal pressure reaches the assigned limit. To start the analysis of the cases, a proper loading path had to be chosen based on the desired outcome. To overcome the lengthy procedure of determining the proper paths experimentally, and since this is a non-linear problem with large deformations, several runs were executed with ANSYS. The initial runs were

utilized to determine the range of the best loading paths that would cause the sample to deform without failure. The loading essentially started with increasing the internal pressure only without any axial feeding to get a quantitative understanding of the behavior of the deformation. Subsequently, the axial movement of the lower edge was given in specific increments. Those results were later utilized in the experimental work. Out of several runs, three pressure ranges were determined to be in the best scope of the hydroforming of the selected specimen. Table 1 shows these ranges, each range of pressure was applied in nine steps for both numerical simulation and experimental work.

Table 1. The selected pressure ranges for the hydroforming

Hydraulic Pressure	Range [MPa]
P_1	0 - 24
P_2	0 - 33.5
P_3	0 - 36.5

There were two phases in the application of the loading configuration for the internal pressure and axial feeding rate. In the first phase, the axial feeding distance was just enough to create a sealing for the internal fluid; therefore, we call this distance the sealing distance, δ. This distance is necessary due to the lateral shortening of the tube after internal pressure is applied. The internal pressure causes the tube to bulge outwards, as well as causing it to shorten as a direct result of the conservation of the material's mass and the applied boundary constraints. This distance was determined directly from ANSYS runs. After determining the shortenings, δ, for each step within each pressure range, more axial feeding was added to the lower edge so that the total axial feeding was according to the following equation,

$$X_i = \delta + Y_i \,. \tag{2}$$

Where X_i is the total axial feeding distance (the movement of the lower edge), and Y_i is the additional distance. The distance increment Y_i was necessary to increase the deformation amount and to force more hydroforming deformation of the tube into the die. The value assigned to it ranged from zero to a maximum value of twice as much as the sealing distance δ, namely, $Y_i = i * \delta$. Where i = {0, 1, 1.5, 2}. This results in the corresponding X_i. Eventually, all the runs were performed for both friction coefficients. For each one of the pressure ranges, the hydroforming process was repeated for all the axial feedings in equation 2.

2.2 Experimental work

Fig. 2 shows the tube hydroforming rig, which was designed and manufactured at the Mechanical Engineering Laboratory of the College of Engineering at Tikrit University. This hydroforming apparatus has the benefit of being versatile in terms of its adaptability by altering a few tooling components. The main part of this rig is the conical die shown in Fig. 3, which gives the shape of the hydroformed tube.

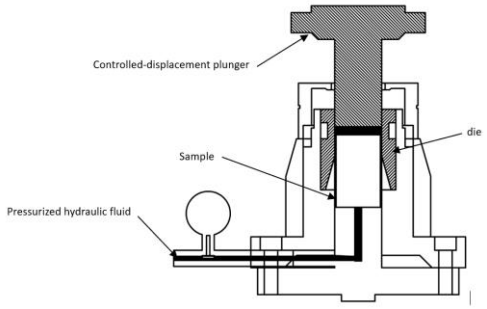

Fig. 2. Schematic drawing of the hydroforming rig

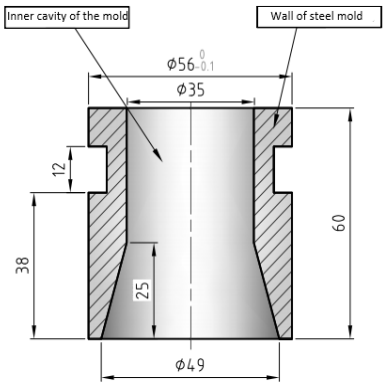

Fig. 3. Schematic drawing of the die

The material used for the tube was copper. To determine the mechanical properties for the material, tensile test was conducted using a universal testing machine (UH-X/FX Shimadzu, 600 kN) shown in Fig. 4.

Fig. 4. Shimadzu, 600 kN Universal testing machine

The tests were conducted according to the ASTM E8/E8M standard. Table 2 shows the mechanical properties of the material. The liquid delivery pump that was used to apply the internal pressure had a capacity of 45 MPa.

Table 2. The mechanical properties of the tubes

Property	Value
Young's modulus	12 GPa
Poisson's ratio	0.35
Yield stress	120 MPa
Strain hardening exponent	0.2
Strength Coefficient	428.87 MPa
Density	8800 kg/m^3

The selected tube pieces had a total length of 60 mm, a diameter of 35 mm, and a thickness of 1 mm. The other details are shown in Fig. 5. Only one end of the tube was open, which was used to deliver the pressurized liquid into the cavity.

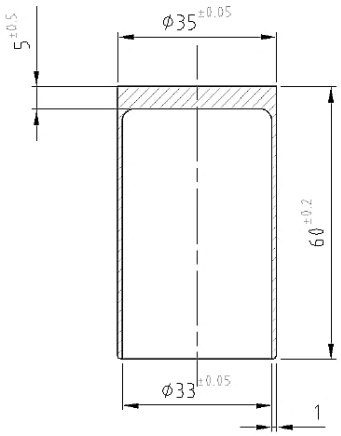

Fig. 5. Geometry of the specimens (dimensions in mm)

3. RESULTS AND DISCUSSION

After running the simulations with the pressure ranges in Table 1 and the two friction coefficients, the results obtained are shown in Fig. 6 for the relationship between the internal pressure and axial feeding for successful hydroforming cases. The results are shown in a two-column format; one for each friction coefficient, and each plotting group shows the results for the application of a pressure range.

For all the plots, the lower curves (blue) represent the axial feeding versus the internal pressure relationship for the case where the axial feeding is barely enough to cap the hydroformed tube's end (X_0), whereas the remaining curves are for the other values of axial feeding. The first observation is that for a range of internal pressure, there was no axial movement. The reason for this is that there is a reciprocal relationship between lateral deformation and longitudinal contraction. However, for the initial application of the pressure (up to ~10 MPa), there was no lateral movement of the tube's end because of the frictional forces. Once the shear forces at the die-specimen interface take over, the tube end starts moving. For axial feedings higher than the sealing axial feedings, $X_{1\text{-}2}$, the shape of the curves was consistent with the expectations – with a slight increase in the amount of the axial feeding with the lower friction coefficient, as can be observed from Fig. 6 A-C for μ = 0.045 and Fig. 6 D-F for μ = 0.03.

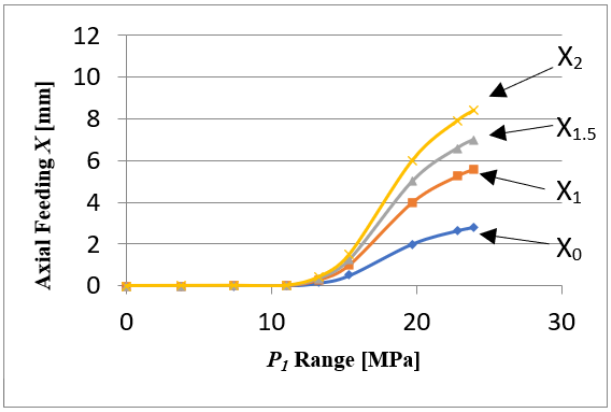

A) P_1 pressure range response

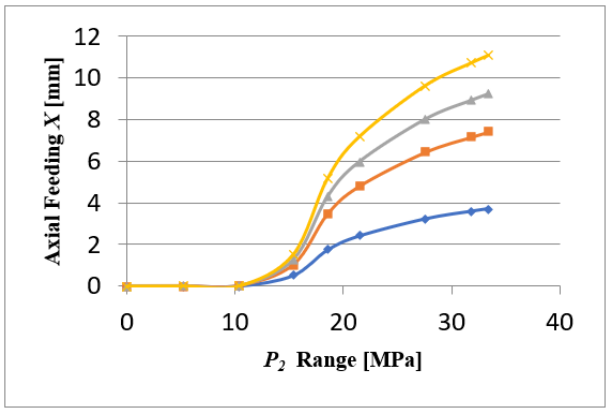

B) P_2 pressure range response

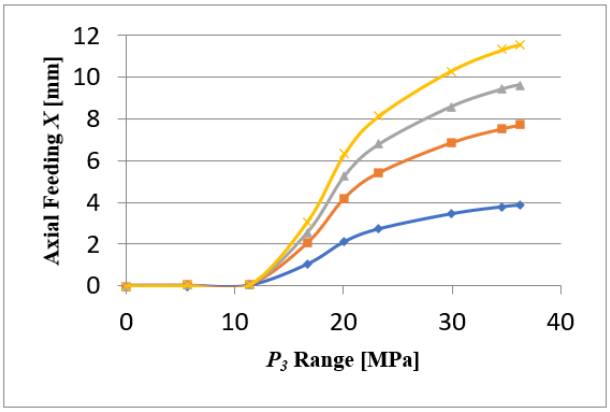

C) P_3 pressure range response

Fig. 6 A-C. Axial feeding – pressure diagrams (for μ = 0.045)

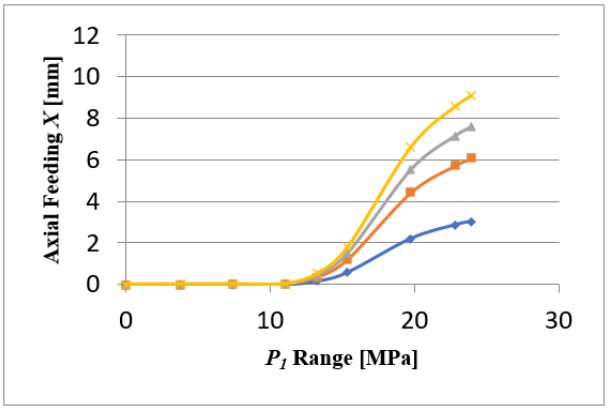

D) P_1 pressure range response

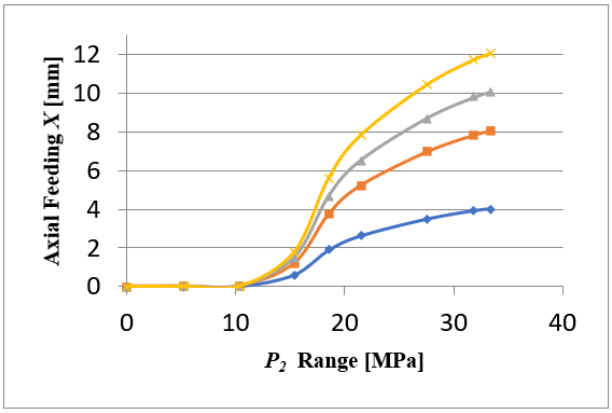

E) P_2 pressure range response

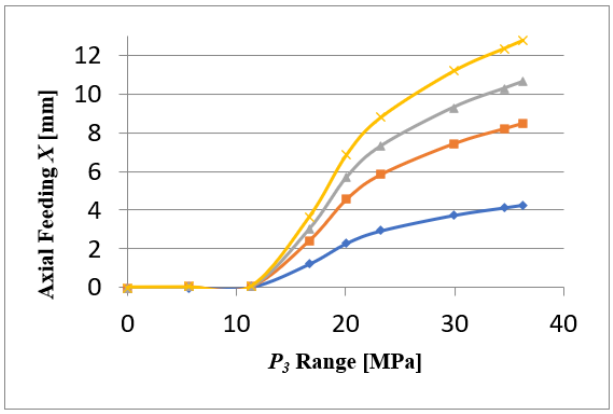

F) P_3 pressure range response

Fig. 6 D-F. Axial feeding – pressure diagrams (for μ = 0.03)

All these axial feeding values have caused the specimen to fill the die's cavity without any failure modes, and it can be noticed that the axial feeding amount increased with the applied pressure range during the nine steps. Furthermore, for each friction coefficient, as the pressure increases and once there is relative movement at the specimen-die interface, the slope of the curves, dX/dP, decreases because the filling of the cavity, including the corner, is reaching its limit. Hence, the highest rate of change happens shortly after the beginning of the relative motion at the specimen-die interface. Furthermore, when the deformation is approaching the limit, the energy spent at this phase might not make a huge difference in terms of the corner fillings and gaps reductions. Although it was possible to have samples with more axial feeding than X_2, it is clear from Fig. 6 that any higher values would only result in small amounts of additional forming. In order to verify that the simulation results were valid, some of them were implemented in the experimental setup with the specimen characterized in Table 1. Initially, some out-of-range cases were tried to check the failure modes. Fig. 7 shows one of such results in which the hydroformed tube was wrinkled after giving more end movement value than what the internal pressure could have compensated by lateral expansion. The bursting failure mode could not be obtained with the current geometric configuration of the setup and with the relatively high ductility of the tube's material.

Fig. 7. Wrinkled tube

After that, the successful runs were put in focus in order to get successful hydroforming. By considering the load steps and the proper timing of pressure application, Fig. 8 shows the experimental result corresponding to the simulation result shown in Fig. 6-C for X_2. The right-hand part of Fig. 8 shows the original tube prior to the process. Then the succeeding ones are the hydroformed tubes at the nine loading stages. For each loading stage, a new tube was used to reach the pressure of that particular step, then was taken out of the testing rig for observation and assessment. It can be noticed that even though this was the highest pressure with the highest end-feeding, the hydroforming was successful with the intended shape. As a result of this, it was concluded that the finite element procedure was accurate as theoretical bases for this study.

Fig. 8. The nine steps of conical THF for the case shown in Fig. 6-C for X_2

To assess the quality of the hydroforming, the final shape of the specimen must be studied. Fig. 9 shows the last six steps for the loading paths that correspond to the one shown in Fig. 6-B for $X_{1.5}$. For the purpose of this work, the quality of the resulting shape was quantified by studying both Δ_1 and Δ_2, which are shown in Fig. 9. These two gap readings represent the result of defects of two different regions of the plastic deformation, with two individual characteristics. At the end of each loading path, gap Δ_1 is the maximum gap between the die's surface and the outer surface of the tube wall at the die's entrance. This gap results due to the effect of the plastic bending as well as the support caused by the lower corner of the die [23]. On the other hand, Δ_2 is the maximum gap between the surface of the tube and the corner of the die. The process of forming the two gaps is demonstrated as follows:

1. As a result of internal hydraulic pressure, the tube wall bulged without circumferential constraint, while at the same time, the axial feeding causes plastic bending at the entrance of die, Fig. (9-A).
2. After that, the contact between the tube wall and the internal surface of the die appears in the form of the Δ_1 gap between two contact points, Fig. (9-B).
3. Increasing the contact area due to both pressure and axial feeding without drawing the wall toward the cone base causes the gaps to be maximum at this step, Fig. (9-C).
4. Further increasing the hydraulic pressure with the contribution of the axial feeding, the material will be drawn more toward the bases of the gaps, which results in reducing the gap and that will progressively lead to the final gap values; Δ_1 and Δ_2, Fig. (9-D-F).

Fig. 10 gives an insight into gap Δ_1 and how it interacts with the other parameters. As can be noticed, when the axial feeding is X_0, the gap is relatively smaller than when it is X_1. The reason for that is the influence of the internal pressure acting to reduce this gap. However, when the axial feeding starts giving more end-movement, the immediate effect is that there is an increase in the gap since the axial feeding was more than necessary, and, at the same time, it caused the tube to bend inwards due to the friction at the surfaces interface as well as the entrance notching effect. In other words, since the axial feeding was not enough to contribute to the drawing tube wall toward the cone base, it caused the accumulation of material at the die's entrance (Fig. 10 for X_1). Nonetheless, when axial feeding is $X_{1.5}$ or more, the tube tends to overcome the sticking condition at the die-surface interface; at this point the hydraulic pressure draws the wall towards the cone base, which results in the reduction of Δ_1, (Fig. 10 for axial feeding X_2). On the other hand, and by observing Fig. 11, the same axial feeding that was applied initially caused gap Δ_2 to shrink progressively without an intermediate increase. The reason for that is this gap benefits directly from the axial feeding with no bending effect that affected gap Δ_1. Hence, the same axial feeding amount had different influence patterns on both gaps. In the same way, as for the first gap, the second one continuously got smaller as the axial feeding increased.

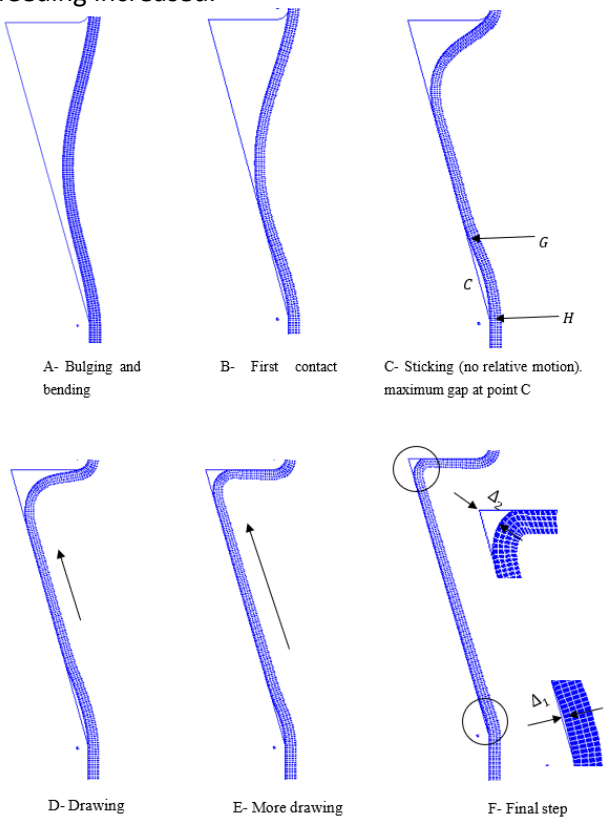

Fig. 9. Deformation mechanism in conical THF

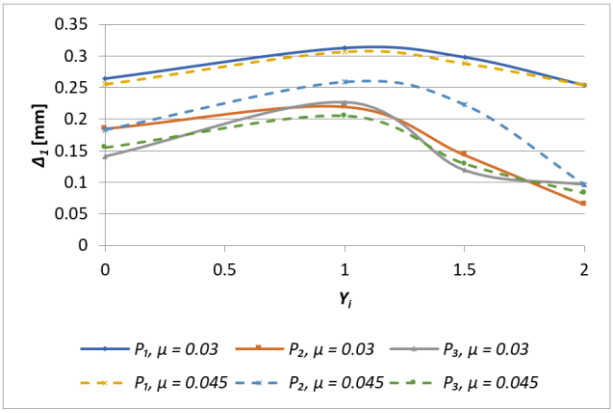

Fig. 10. Variation of Δ_1 with pressure, axial feeding, and coefficient of friction

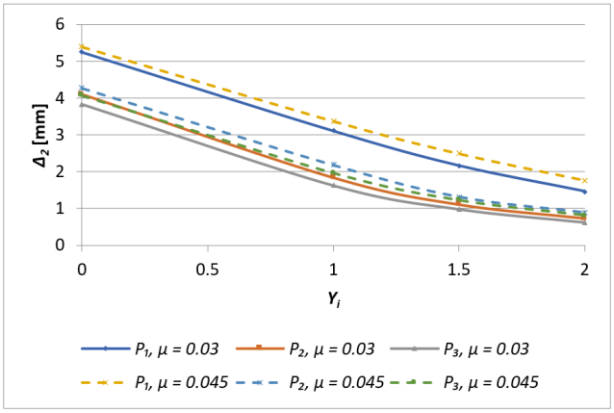

Fig. 11. Variation of Δ_2 with pressure, axial feeding, and coefficient of friction

In regard to the direct effect of friction coefficient on the gaps, Δ_1 and Δ_2 were affected in mixed ways. By studying Fig. 10 and 11, the coefficient of friction caused the gaps to become smaller while enlarging them in other instances. On one hand, for gap Δ_1, it is not clear how to isolate the bending effect coming from the entrance edge. Fig. 9-C shows the contact points (G and H) of this gap which shows potentially variable frictional forces at these points. On the other hand, gap Δ_2 shows apparent proportional behavior in which the lower the friction coefficient, the smaller the gap value. The reason for this is that the material's flow had no restrictions in terms of the bending effect over the corner. This behavior in both gaps highlights the importance of including the bending effect in the hydroforming studies for yielding and failure criteria [23]. It is worth mentioning that Δ_1 closure could be enhanced if there is feeding from both sides of the tube since this would result in reducing the frictional forces impact on the process.

4. CONCLUSION

In this study, twelve load paths were considered for tube hydroforming in a conical die. The simulation results were utilized to study the process at different phases. Then, the results were compared to experimental observations. Here are the main conclusions:

1. The effect of bending at the entrance where the material feeding is given is high and might overcome the frictional forces impact on the process;
2. The highest rate of deformation happens shortly after the die-specimen interface starts having relative motion;
3. The energy consumption at the limiting end of the process is higher than at the beginning. Hence, the design process of the dies should include having most of the required deformation at the beginning;
4. For successful and complete hydroforming, the axial feeding would need to be twice the sealing distance;
5. The inclusion of friction at the die-specimen interface is crucial in hydroforming studies and has mixed impacts on the resulting shape.

REFERENCES

[1] B.G. Marlapalle, R.S. Hingole, Predictions of formability parameters in tube hydroforming process. *SN Applied Sciences*, 3(6), 2021: 606. https://doi.org/10.1007/s42452-021-04533-4

[2] M. Ahmetoglu, T. Altan, Tube hydroforming: state-of-the-art and future trends. *Journal of Materials Processing Technology*, 98(1), 2000: 25–33. https://doi.org/10.1016/S0924-0136(99)00302-7

[3] L.H. Lang, Z.R. Wang, D.C. Kang, S.J. Yuan, S.H. Zhang, J. Danckert, K.B. Nielsen, Hydroforming highlights: sheet hydroforming and tube hydroforming. *Journal of Materials Processing Technology*, 151(1), 2004: 165-177. https://doi.org/10.1016/j.jmatprotec.2004.04.032

[4] G. Ngaile, Hydroforming Tribology, In: Q.J. Wang, Y.W. Chung, (Ed.), Encyclopedia of Tribology. *Springer*, US, 2013, pp.1765-1774.

[5] S. Milojević, D. Gročić, D. Dragojlović, CNG propulsion system for reducing noise of existing city buses. *Journal of Applied Engineering Science*, 14(3), 2016: 377-382. https://doi.org/10.5937/jaes14-10991

[6] S. Milojević, S. Savić, D. Marić, O. Stopka, B. Krstić, B. Stojanović, Correlation between Emission and Combustion Characteristics with the Compression Ratio and Fuel Injection Timing in Tribologically Optimized Diesel Engine. *Tehnički Vjesnik*, 29(4), 2022: 1210–1219. https://doi.org/10.17559/TV-20211220232130

[7] S. Milojević, B. Stojanović, Determination of tribological properties of aluminum cylinder by application of Taguchi method and ANN-based model. *Journal of the Brazilian Society*

of Mechanical Sciences and Engineering, 40(12), 2018: 571. https://doi.org/10.1007/s40430-018-1495-8

[8] L. Sun, C. Lin, Z. Fan, H. Li, G. Wang, G. Chu, Multistage Axial Hydro-Forging Sequence: A New Forming Approach for Manufacturing of Double-Stepped Tubes. *Journal of Materials Engineering and Performance*, 28(11), 2019: 6800-6808. https://doi.org/10.1007/s11665-019-04444-x

[9] M. Jansson, L. Nilsson, K. Simonsson, On strain localisation in tube hydroforming of aluminium extrusions. *Journal of Materials Processing Technology*, 195(1), 2008: 3-14. https://doi.org/10.1016/j.jmatprotec.2007.05.040

[10] S. Kim, Y. Kim, Analytical study for tube hydroforming. *Journal of Materials Processing Technology*, 128(1), 2002: 232-239. https://doi.org/10.1016/S0924-0136(02)00456-9

[11] L. Galdos, J. Trinidad, N. Otegi, C. Garcia, Friction Modelling for Tube Hydroforming Processes - A Numerical and Experimental Study with Different Viscosity Lubricants. *Materials*, 15(16), 2022: 5655. https://doi.org/10.3390/ma15165655

[12] F. Mohammadi, M.M. Mashadi, Determination of the loading path for tube hydroforming process of a copper joint using a fuzzy controller. *The International Journal of Advanced Manufacturing Technology*, 43(1), 2009: 1-10. https://doi.org/10.1007/s00170-008-1697-9

[13] L. Shu-hui, B. Yang, Z. Wei-gang, L. Zhong-qin, Loading path prediction for tube hydroforming process using a fuzzy control strategy. *Materials & Design*, 29(6), 2008: 1110-1116. https://doi.org/10.1016/j.matdes.2007.06.008

[14] C. Zhang, W. Liu, L. Huang, C. Wang, H. Huang, L. Lin, P. Wang, Process analysis of biconvex tube hydroforming based on loading path optimization by response surface method. *The International Journal of Advanced Manufacturing Technology*, 112(9), 2021: 2609-2622. https://doi.org/10.1007/s00170-020-06411-6

[15] S.L. Lin, F.K. Chen, Die Design and Axial Feeding in the Tube-Hydroforming Process, ASME 2010 International Manufacturing Science and Engineering Conference. American Society of Mechanical Engineers Digital Collection, October 12-15, 2010, Erie, Pennsylvania, USA, pp. 619-622. https://doi.org/10.1115/MSEC2010-34113

[16] Y. Jia, J. Li, J. Luo, Analysis and experiment on tube hydroforming in a rectangular cross-sectional die. *Advances in Mechanical Engineering*, 9(5), 2017: 1687814017694831. https://doi.org/10.1177/1687814017694831

[17] C. Qi, L. Yan, S. Yang, S. Yuan, An optimization procedure for concave preform design in rectangular tube hydroforming. *The International Journal of Advanced Manufacturing Technology*, 120(7), 2022: 5311-5324. https://doi.org/10.1007/s00170-022-09080-9

[18] S.L. Lin, Z.W. Chen, F.K. Chen, A study on localized expansion defects in tube hydroforming. *Journal of the Chinese Institute of Engineers*, 41(2), 2018: 149-159. https://doi.org/10.1080/02533839.2018.1437367

[19] C.P. Nikhare, T. Buddi, N. Kotkunde, S.K. Singh, Effect of Die Velocity on Tube Deformation Mechanics During Low Pressure Tube Hydroforming Process Sequence Variation. *International Mechanical Engineering Congress and Exposition. American Society of Mechanical Engineers Digital Collection - ASME 2021*, November 1-5, 2021, Virtual, Online, V02AT02A051. https://doi.org/10.1115/IMECE2021-70179

[20] P.V. Reddy, B.V. Reddy, P.J. Ramulu, An investigation on tube hydroforming process considering the effect of frictional coefficient and corner radius. *Advances in Materials and Processing Technologies*, 6(1), 2020: 84-103. https://doi.org/10.1080/2374068X.2019.1707437

[21] H. Orban, S.J. Hu, Analytical modeling of wall thinning during corner filling in structural tube hydroforming. *Journal of Materials Processing Tech*, 1–3(194), 2007: 7-14. https://doi.org/10.1016/j.jmatprotec.2007.03.112

[22] G.T. Kridli, L. Bao, P,K, Mallick, Y. Tian, Investigation of thickness variation and corner filling in tube hydroforming. *Journal of Materials Processing Tech*, 3(133), 2003: 287-296. https://doi.org/10.1016/S0924-0136(02)01004-X

[23] C. Yang, G. Ngaile, Analytical model for planar tube hydroforming: Prediction of formed

shape, corner fill, wall thinning, and forming pressure. *International Journal of Mechanical Sciences*, 50(8), 2008: 1263-1279. https://doi.org/10.1016/j.ijmecsci.2008.05.006

[24] M. Jansson, L. Nilsson, K. Simonsson, Tube hydroforming of aluminium extrusions using a conical die and extensive feeding. *Journal of Materials Processing Technology*, 198(1), 2008: 14-21. https://doi.org/10.1016/j.jmatprotec.2007.09.043

[25] M.D. M, Experimental and Finite Element Study of the Hydroforming Bi-layered Tubular Component (Master's Thesis). *Dublin City University*, Ireland, 2005.

[26] J.Y. Chen, Z.C. Xia, S.C. Tang, Corner Fill Modeling of Tube Hydroforming, ASME 2000 International Mechanical Engineering Congress and Exposition. American Society of Mechanical Engineers Digital Collection, November 5-10, 2000, Orlando, Florida, USA, pp. 635-640. https://doi.org/10.1115/IMECE2000-1863

[27] Y.M. Hwang, T. Altan, Finite element analysis of tube hydroforming processes in a rectangular die. *Finite Elements in Analysis and Design*, 39(11), 2003: 1071-1082. https://doi.org/10.1016/S0168-874X(02)00157-9

[28] B.V. Reddy, D. Kondayya, E.V. Goud, P.V. Reddy, Yield criterion influence on the formability prediction of SS 304 by tensile tests and bulge tests during tube hydroforming process. *Multiscale and Multidisciplinary Modeling, Experiments and Design*, 4(4), 2021: 293–302. https://doi.org/10.1007/s41939-021-00096-4

[29] A.T. Male, M.G. Cockcroft, A Method for the Determination of the Coefficient of Friction of Metals under Conditions of Bulk Plastic Deformation. *Journal Institute of Metals*, 93(38), 1964: 93-98.